Cancer Chemother Pharmacol (2008) 62:799–808
DOI 10.1007/s00280-007-0667-5

ORIGINAL ARTICLE

7-Chloro-6-piperidin-1-yl-quinoline-5,8-dione (PT-262), a novel synthetic compound induces lung carcinoma cell death associated with inhibiting ERK and CDC2 phosphorylation via a p53-independent pathway

Tzu-Sheng Hsu · Chinpiao Chen · Pei-Ting Lee · Shu-Jun Chiu · Huei-Fang Liu · Chih-Chien Tsai · Jui-I Chao

Received: 15 August 2007 / Accepted: 17 December 2007 / Published online: 10 January 2008

Abstract
Background The derivatives of 5,8-quinolinedione have been shown to exert anticancer activities. A new synthetic compound 7-chloro-6-piperidin-1-yl-quinoline-5,8-dione (designed as PT-262) derived from 6,7-dichloroquinoline-5,8-dione on its anticancer activity was investigated in this study.
Materials and methods PT-262 was synthesized as the following: triethylamine (0.56 ml, 5.1 mmol) was added dropwise to a solution of 6,7-dichloroquinoline-5,8-dione (1.00 g, 4.4 mmol) and piperidine (0.50 ml, 5.1 mmol) in 150 ml of benzene with stirring at room temperature for 5 min, and the solvent was removed using rotary evaporator to give a dark brown solid. PT-262 was purified by flash chromatography using 50% ethyl acetate/hexanes to elute that displayed as brown solids. To examine the induction of apoptosis following PT-262 treatment, the lung cancer cells were subjected to apoptotic cell observation, caspase activation, and mitochondrial functional assays. The protein levels of phosphorylated ERK and CDC2 after treatment with PT-262 were analyzed by Western blot.
Results Treatment with 1–20 μM PT-262 for 24 h induced cytotoxicity via a concentration-dependent manner in human lung cancer cells. PT-262 induced the loss of mitochondrial membrane potential and elevated the caspase-3 activation and apoptosis. Interestingly, the phosphorylation of ERK was inhibited by PT-262. The IC_{50} value of ERK phosphorylation inhibition was approximate around 5 μM. Treatment with a specific MEK1/2 (the upstream of ERK) inhibitor, PD98059, increased the PT-262-induced cytotoxicity in lung cancer cells. Moreover, PT-262 did not alter the protein expression of tumor suppressor p53. PT-262 elicited the cytotoxicity and accumulated the G_2/M fractions in both the p53-wild type and p53-null lung cancer cells. The mitosis-regulated protein levels of cyclin B1 and phospho-CDC2 at Thr14, Tyr15, and Thr161 were repressed by PT-262 in these cells.
Conclusion PT-262 suppresses the phosphorylation of ERK and CDC2 associated with proliferation inhibition via a p53-independent pathway in human lung cancer cells.

Keywords Apoptosis · CDC2 · ERK · p53 · PT-262 · 5,8-quinolinedione

Abbreviations

MAP	Mitogen-activated protein
ERK	Extracellular signal-regulated kinase
CDKs	Cyclin-dependent protein kinases
F-actin	Actin filament
PI	Propidium iodide
MTT	3-(4,5-Dimethyl-thiazol-2-yl) 2,5-diphenyl tetrazolium bromide
DMSO	Dimethyl sulfoxide
FBS	Fetal bovine serum
PBS	Phosphate-buffered saline

Electronic supplementary material The online version of this article (doi:10.1007/s00280-007-0667-5) contains supplementary material, which is available to authorized users.

T.-S. Hsu · H.-F. Liu · C.-C. Tsai · J.-I. Chao (✉)
Institute of Pharmacology and Toxicology,
Tzu Chi University, 701, Section 3,
Chung-Yang Road, Hualien 970, Taiwan
e-mail: chaoji@mail.tcu.edu.tw

C. Chen · P.-T. Lee
Department of Chemistry,
National Dong Hwa University, Hualien, Taiwan

S.-J. Chiu
Department of Life Science, Tzu Chi University,
Hualien, Taiwan

Introduction

The 5,8-quinolinediones and 6,7-dihaloquinoline-5,8-diones are useful precursors for producing multiple types of bioactive products [1]. The derivatives of quinolinediones have been shown to possess many biological activities including antitumor and antimicrobial actions [2–6]. It has been shown that 6-anilino-5,8-quinolinedione (LY83583), an inhibitor of guanylyl cyclase, inhibits cell proliferation in tumor cells [5, 6]. 6-Chloro-7-(2-morpholin-4-yl-ethylamino)quinoline-5,8-dione (NSC 663284), a potent inhibitor of CDC25 protein phosphatases, blocks the proliferation of human breast cancer cells [3, 7]. In addition, lavendamycin is a bacterially derived quinolinedione that displays significant antitumor activity [4]. Therefore, the different quinolinedione compounds may exert their anticancer activity through varied anticancer target proteins or enzymes in cancer cells.

The blockade of survival pathways and the induction of apoptotic pathways in cancer cells are the important strategies in cancer therapy [8–10]. It has been shown that mitogen-activated protein (MAP) kinase pathways regulate various cellular physiologic events including cell proliferation, survival, growth arrest, and apoptosis [11]. Extracellular signal regulated-protein kinase (ERK) is the important signal pathway to control cancer cell proliferation and transformation [12, 13]. Moreover, the activation of ERK plays a critical role in cell adhesion and motility [14]. In contrast, p53, a tumor suppressor protein, mediates the cell cycle arrest and promotes apoptosis in cancer cells resulting in the prevention of cancer development [15–17]. Anticancer agents may apply to their activities through the induction of apoptosis or the inhibition of proliferation in tumor cells [6, 10, 18]. However, numerous cancer cells contain the mutations of p53, which resist to the chemotherapy of cancers. Thus, the development of anticancer drugs for treatment on the p53-mutational cancers is highly desired.

The cell cycle arrest mediated by inappropriate activity of the cyclin-dependent protein kinases (CDKs) can trigger growth inhibition and apoptosis in cancer cells [3, 19, 20]. The CDK1 (CDC2) interacts with cyclin B1 that has been shown to play a critical role in the mitotic progression [20–22]. The formation of CDC2/cyclin B1 complexes is required for G_2 into mitosis [21, 22]. It has been shown that G_2/M phase arrest is exhibited in cells exposed to a variety of anticancer agents [23–25]. For example, NSC 663284 can block the CDC25C phosphatase resulting in the decrease of CDC2 kinase activity for inducing the cell cycle arrest in cancer cells [7].

7-Chloro-6-piperidin-1-yl-quinoline-5,8-dione, a new derivative of 5,8-quinolinedione, is designated as PT-262. Among new synthetic compounds in this study, PT-262 is the most potent to induce lung cancer cell death. Interestingly, PT-262 inhibits the ERK and CDC2 phosphorylation and induces the G_2/M arrest in lung cancer cells. Moreover, PT-262 is effective to induce proliferation inhibition and cell cycle arrest in both p53-wild type and p53-null cancer cells. These findings indicate that PT-262 induces cancer cell death and growth inhibition via a p53-independent pathway.

Materials and methods

Synthesis and chemical property of PT-262

Briefly, triethylamine (0.56 ml, 5.1 mmol) was added dropwise to a solution of 6,7-dichloroquinoline-5,8-dione (1.00 g, 4.4 mmol) and piperidine (0.50 ml, 5.1 mmol) in 150 ml of benzene with stirring at room temperature for 5 min, and the solvent was removed using rotary evaporator to give a dark brown solid. PT-262 was purified by flash chromatography using 50% ethyl acetate/hexanes to elute that displayed as brown solids. The property of PT-262 is as follows: mp 145–146°C; ^{1}H NMR (300.1 MHz, $CDCl_3$, δ): 9.00 (dd, J = 4.7, 1.7 Hz, 1H), 8.34 (dd, J = 7.9, 1.7 Hz, 1H), 7.60 (dd, J = 7.9, 4.7 Hz, 1H), 3.57 (t, J = 5.1 Hz, 4H), 1.79–1.76 (m, 6H). ^{13}C NMR (125.7 MHz, $CDCl_3$, δ): 180.6, 175.7, 154.0, 149.5, 146.6, 134.3, 127.5, 126.5, 122.1, 52.5, 26.3, 23.4; IR (KBr) cm^{-1}: 2935, 2849, 1690, 1643, 1589, 1558, 1294, 836, 722; MS m/z: 277 (M^+ + 1, 36), 154 (100), 136 (83), 55 (80), 93 (31); high resolution MS (m/z): $C_{14}H_{13}ClN_2O_2$, 276.0666. The preparation procedures and MS and NMR spectra for other compounds were presented in the supplementary information. All the compounds were dissolved in 100% dimethyl sulfoxide (DMSO). The concentration of DMSO was <0.2% in the control and drug-containing media in each experiment.

Reagents and antibodies

Hoechst 33258, propidium iodide (PI), 3-(4,5-dimethylthiazol-2-yl) 2,5-diphenyl tetrazolium bromide (MTT), and the Cy3-labeled mouse anti-β-tubulin were purchased from Sigma Chemical Co. (St. Louis, MO, USA). BODIPY FL phallacidin was purchased from Molecular Probes Co. (Eugene, OR, USA). Anti-phospho-CDC2 (Thr-161) (9114S), anti-phospho-CDC2 (Thr14) (#2543), anti-phospho-CDC2 (Tyr15) (#4539), and anti-phospho-ERK (9101S) were purchased from Cell Signaling Technology Inc. (Beverly, MA, USA). Anti-ERK-2 (C-14) and anti-cyclin D1 were purchased from Santa Cruz Biotechnology, Inc. (Santa Cruz, CA, USA). Anti-p21 (Ab-1), anti-CDC2 (Ab-1), and anti-cyclin B1 (Ab-2) were purchased from Oncogene Sciences (Cambridge, MA, USA). Anti-caspase-3 (3004–100) was purchased from BioVision Research

Products (Mountain View, CA, USA). 2′-Amino-3′-methoxyflavone (PD98059) was purchased from Calbiochem (San Diego, CA, USA).

Cell culture

The A549 cell line (ATCC, #CCL-185) was derived from lung carcinoma that contained the wild type p53. The H1299 cell line (ATCC, #CRL-5803) has a homozygous deletion of the *p53* gene that was derived from a non-small cell lung adenocarcinoma tumor. These cell lines were cultured in complete RPMI-1640 medium (Gibco, Life Technologies, Grand Island, NY, USA) supplemented with 10% fetal bovine serum (FBS), 100 units/ml penicillin, 100 μg/ml streptomycin, and L-glutamine (0.03%, w/v), and cells were incubated at 37°C and 5% CO_2.

Cytotoxicity assay

Briefly, the cells were plated in 96-well plates at a density of 1×10^4 cells/well for 16–20 h. Then the cells were treated with or without PT-262 for 24 h in RPMI-1640 medium. After drug treatment, the cells were washed with phosphate-buffered saline (PBS), and were re-cultured in complete RPMI-1640 medium for 2 days. Thereafter, the medium was replaced and the cells were incubated with 0.5 mg/ml of MTT reagent in complete RPMI-1640 medium for 4 h. The surviving cells converted MTT to formazan that generates a blue-purple color when dissolved in DMSO. The intensity of formazan was measured at 565 nm using a plate reader (Molecular Dynamics, OPTImax) for enzyme-linked immunosorbent assays. Cell viability was calculated by dividing the absorbance of treated cells by that of the control in each experiment.

Cell number analysis

The cells were plated at a density of 5×10^5 cells per 100-mm Petri dish in complete RPMI-1640 medium for 16–20 h. Then the cells were treated with 0–10 μM PT-261 or PT-262 for 24 h. After drug treatment, the cells were washed twice with PBS and re-cultured in complete RPMI-1640 medium. The cells were re-cultured for 1–5 days before they were counted by a hemocytometer.

Apoptosis assay

A549 cells were cultured on coverslip in a 60-mm Petri dish for 16–20 h before treatment. After treatment with PT-262, the cells were carefully washed with isotonic PBS (pH 7.4), and incubated with 4% paraformaldehyde solution in PBS for 1 h at 37°C. The F-actin and β-tubulin were stained with 20 U/ml BODIPY FL phallacidin and anti-β-tubulin Cy3 (1:50) for 30 min at 37°C, respectively. The nuclei were stained with 2.5 μg/ml Hoechst 33258 for 30 min at room temperature. The number of apoptotic nuclei was counted by a hemocytometer under a fluorescence microscope. The cell morphology of apoptosis was confirmed by observation of the formation of apoptotic nuclei and bodies. Five hundred cells were counted in each experiment for the calculation of apoptotic percentage.

Mitochondrial membrane potential

Briefly, A549 cells were cultured in 60-mm Petri dish at a density of 5×10^5 cells. At the end of treatment, the cells were washed with ice-cold PBS and were trypsinized. The cells were collected by centrifugation, and the pellets were resuspended in 70% ethanol and stored at −20°C for 2 h. After centrifugation, the pellets were incubated with 500 nM DiOC6 at 37°C for 30 min. Finally, the cell pellets were collected by centrifugation and resuspended in 0.5 ml ice-cold PBS. The fluorescence intensities of DiOC6 were analyzed by a flow cytometer (FACScan, Becton Dickinson, San Jose, CA, USA).

Western blot analysis

At the end of treatment, the cells were lysed in the ice-cold whole cell extract buffer containing the protease inhibitors as described [20]. Western analyses of cyclin B1, cyclin D1, CDC2, phospho-CDC2 (Thr14), phospho-CDC2 (Tyr15), phospho-CDC2 (Thr161), p53, p21, caspase-3, phospho-ERK, and ERK-2 were performed using specific antibodies. Briefly, equal amounts of proteins in samples were subjected to electrophoresis using 10–12% sodium dodecyl sulfate-polyacrylamide gels. After electrophoretic transfer of proteins onto polyvinylidene difluoride membranes, they were sequentially hybridized with primary antibody and followed with a horseradish peroxidase-conjugated secondary antibody (Santa Cruz Biotechnology, Inc., Santa Cruz, CA, USA). Finally, the protein bands were visualized using the enhanced chemiluminescence detection system (PerkinElmer Life Sciences). The software of Un-Scan-It *gel* (Ver. 5.1, Silk Scientific, Inc.) was used to quantify the intensity of each band.

Cell cycle assay

To examine the effect of PT-262 on the cell cycle progression, A549 or H1299 cells were plated at a density of 1×10^6 cells per 60-mm dish in complete RPMI-1640 medium for 16–20 h. Then the cells were treated with 0–10 μM PT-262 for 24 h. At the end of the treatment, cells were collected and fixed with ice-cold 70% ethanol and stored at −20°C for overnight. After centrifugation,

the cell pellets were incubated with 4 μg/ml PI solution containing 1% Triton X-100 and 100 μg/ml RNase for 30 min. To avoid cell aggregation, the cell solutions were filtered through nylon membrane (Becton-Dickinson, San Jose, CA, USA). The samples were analyzed by a flow cytometer (FACScan, Becton Dickinson, San Jose, CA, USA) using Cell Quest software. The 10,000 cells were analyzed, and the percentage of cell cycle phases was quantified by a ModFit LT software (Ver. 2.0, Becton-Dickinson).

Statistical analysis

All results were obtained at least from three separate experiments. Data were analyzed by one-way analysis of variance (ANOVA), and further post-hoc tests using the statistic software of GraphPad Prism 4 (GraphPad software, Inc. San Diego, CA, USA). Differences among control and PT-262 treated samples were compared by one-way ANOVA with post-hoc Tukey's tests. A p value of <0.05 was considered as statistically significant.

Results

PT-262 induces cytotoxicity and proliferation inhibition in human lung cancer cells

The chemical structures of 5,8-quinolinedione derivatives or analogues are shown in Fig. 1a. Among these new synthetic compounds, the compound 3 was the most potent to induce cell death in human A549 lung cancer cells (Fig. 1b, c). The compound 3 was designated as PT-262. The compound 2 (designated as PT-261), an isomer of PT-262, and other compounds did not significantly induce cytotoxicity at the concentrations 10 and 40 μM for 24 h in A549 cells (Fig. 1b, c). Treatment with 5–40 μM PT-262 for 24 h reduced the cell viability via a concentration-dependent manner in A549 cells. The value of IC_{50} (the concentration of 50% inhibition of cell viability) was around 5 μM (Fig. 2). However, the IC_{50} value of PT-262 toward human normal lung fibroblast was >20 μM (data not shown). Moreover, PT-262 reduced the total cell number in A549 cells (Fig. 3). Treatment with 10 μM PT-262 for 24 h

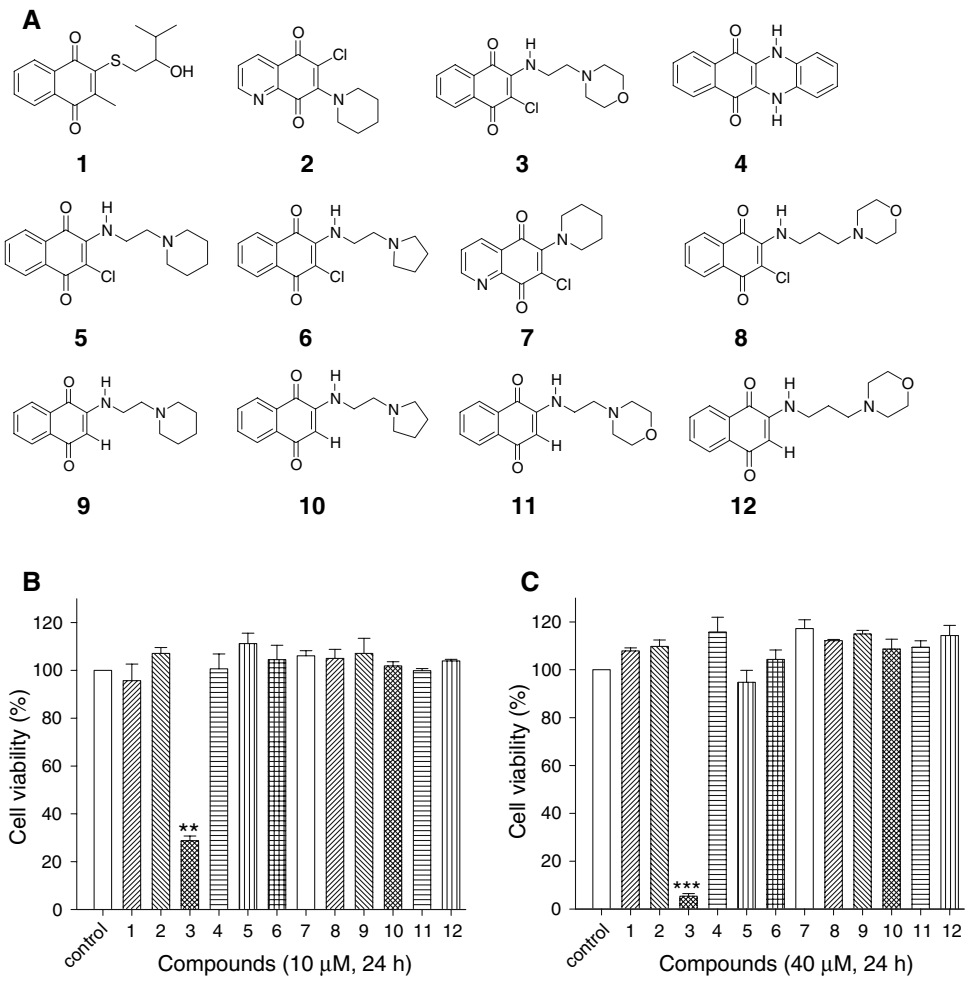

Fig. 1 A variety of 5,8-quinolinediones derivatives or analogues on the cytotoxicity in human lung cancer cells. (**a**) Chemical structure of 5,8-quinolinediones derivatives or analogues. (**b**), (**c**), A549 lung cancer cells were treated with compounds (10 or 40 μM for 24 h). After treatment, the cells were washed twice with PBS, and were re-cultured in fresh medium for 48 h. The cell viability was measured by MTT assay. Results were obtained from 3 to 14 experiments and the bar represents the mean ± S.E. $p < 0.01$ (**) and $p < 0.001$ (***), indicate significant difference between the control and drug treated samples

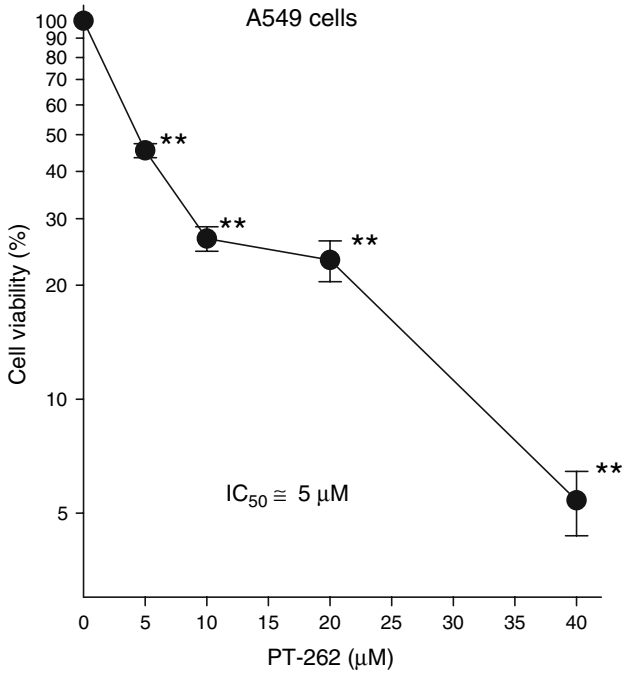

Fig. 2 The IC_{50} value of PT-262 in human lung cancer cells. A549 cells were treated with or without 5–40 μM PT-262 for 24 h. After treatment, the cells were washed twice with PBS, and were re-cultured in fresh medium for 48 h. The cell viability was measured by MTT assay. Results were obtained from 4 to 10 experiments and the *bar* represents the mean ± S.E. $p < 0.01$ (**), indicates significant differences between the control and PT-262 treated samples

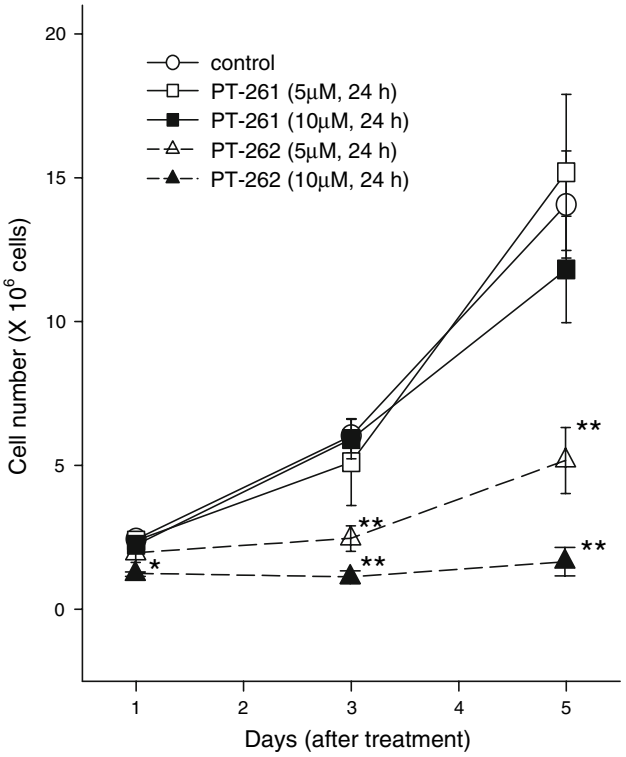

Fig. 3 The effect of PT-261 and PT-262 on the cell proliferation in lung carcinoma cells. A549 cells were plated at a density of 5×10^5 cells/p100 Petri dish for 18 h. Thereafter, the cells were treated with 5 or 10 μM PT-261 and PT-262 for 24 h. After drug treatment, the cells were washed with PBS, and incubated for various times before they were counted by a hemocytometer. Results were obtained from three experiments and the *bar* represents the mean ± S.E. $p < 0.05$ (*) and $p < 0.01$ (**), indicate significant differences between the control and PT-262 treated samples

almost completely blocked the cell proliferation, but PT-261 did not exert the proliferation inhibition (Fig. 3).

PT-262 induces caspase-3 activation, mitochondrial dysfunction and apoptosis in lung cancer cells

To examine the induction of apoptosis following PT-262 treatment, the lung cancer cells were subjected to apoptotic cell observation, caspase activation, and mitochondrial functional assays. The apoptotic morphology after treatment with PT-262 was observed by phase contrast microscopy. The arrows indicated the apoptotic cells induced by PT-262 in A549 cells (Fig. 4a, *arrows*). The apoptotic cells were increased after treatment with PT-262 at 10 μM for 8–24 h (Fig. 4a). The active forms of caspase-3 (12 and 17 kD) were induced following treatment with 2–20 μM PT-262 for 24 h (Fig. 4b). ERK-2 protein has been used as an internal control protein in several studies [20, 26]. The protein levels of ERK-2 were not altered by PT-262. Moreover, PT-262 induced the loss of mitochondrial membrane potential (Fig. 4c). Further, to count the apoptotic cell number after treatment with PT-262, lung cancer cells were subjected to nuclear and cytoskeletal staining. An example of apoptotic nuclear fragments was observed by treatment with PT-262 in an A549 cell (Fig. 4d, *arrows*). The apoptotic cells presented that the cytoskeleton of F-actin (green color) and *β*-tubulin (red color) was disrupted (Fig. 4d). Counting the apoptotic cells, the number of apoptotic events was increased after treatment with 2–10 μM PT-262 for 24 h (Fig. 4d).

PT-262 represses ERK phosphorylation in lung cancer cells

The chemical structure of PD98059 is shown in Fig. 5a. PD98059 is a specific inhibitor of MEK1/2, the upstream kinases of ERK1/2. Treatment with 2–10 μM PD98059 for 24 h significantly inhibited the phosphorylation of ERK1/2 in A549 cells (Fig. 5b). Also, the protein levels of phospho-ERK were decreased via a concentration-dependent manner after treatment with 2–10 μM PT-262 for 24 h (Fig. 5c). The phosphorylation of ERK proteins included two bands that indicated ERK-1 (44 kDa) and ERK-2 (42 kDa). Quantification of Western blots showed that treatment with PT-262 and PD98059 (2–10 μM for 24 h) significantly inhibited the phosphorylation of ERK (Fig. 5d). Moreover, treatment with PD98059 (50 μM for 2 h) or PT-262 (8 μM

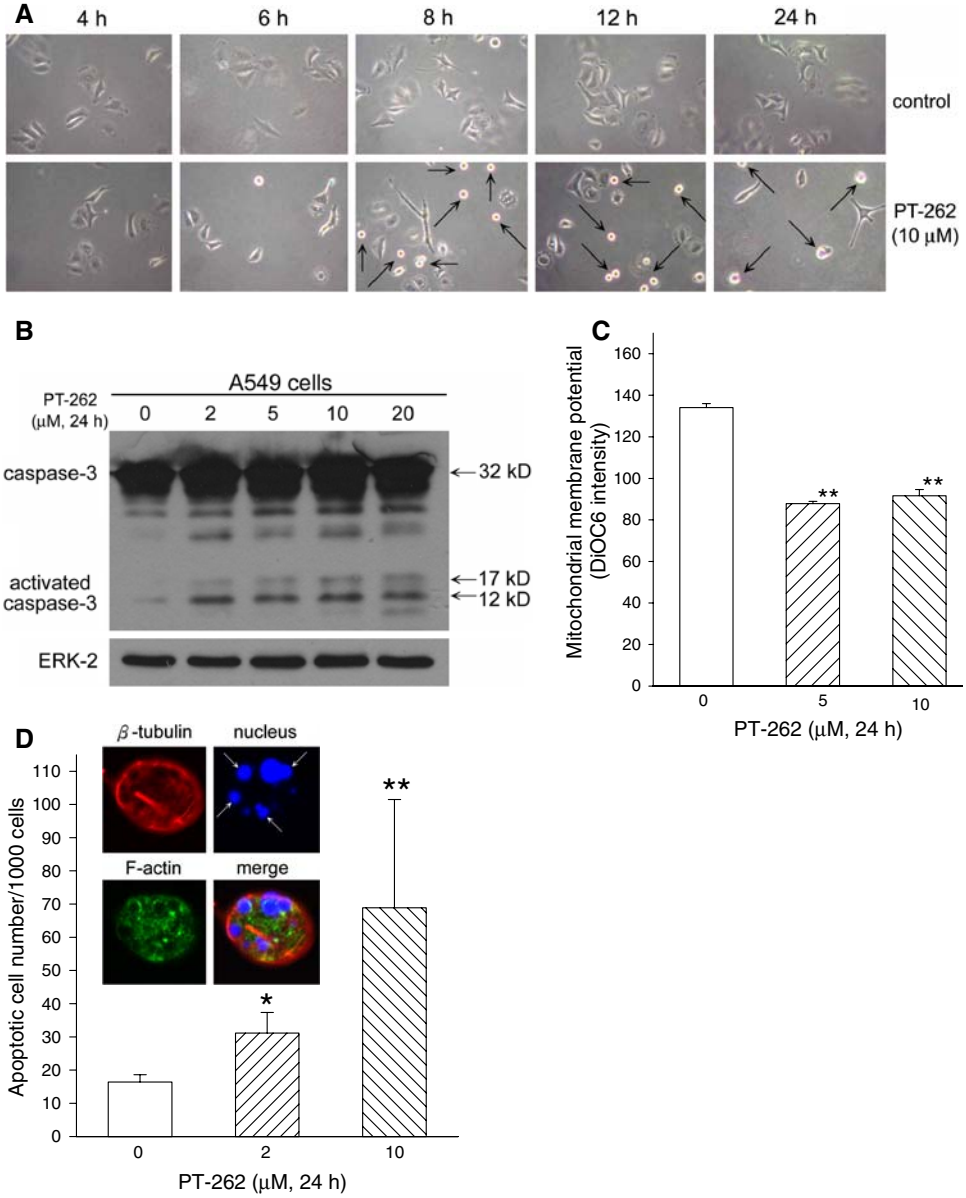

Fig. 4 The effect of PT-262 on the apoptotic induction in lung carcinoma cells. **a** A549 cells were treated with or without 10 μM PT-262 for 4–24 h. The cells were observed under a phase contrast microscope. The *arrows* indicated the apoptotic cells. **b** The total protein extracts were subjected to Western blot analysis by using anti-caspase-3 and anti-ERK-2 antibodies. Representative Western blot results were shown from 1 of 3 separate experiments with similar findings. **c** Mitochondrial membrane potential was evaluated by flow cytometry analysis of cells stained with DiOC6. Results were obtained from 3 to 4 experiments and the *bar* represents mean ± S.E. $p < 0.01$ (**), indicates significant differences between control and PT-262 treated samples in A549 cells. **d** The *β*-tubulin, F-actin, and nuclei were stained with the Cy3-labeled mouse anti-*β*-tubulin, BODIPY FL phallacidin, Hoechst 33258, respectively. *Arrows* indicate the nuclear fragments in a PT-262-treated cell. After treatment with or without PT-262, the apoptotic cell number was scored. Results were obtained from three experiments and the *bar* represents mean ± S.E. $p < 0.05$ (*), indicates significant differences between control and PT-262 treated samples

for 24 h) significantly reduced cell viability in A549 cells (Fig. 6). Besides, combination with PD98059 and PT-262 additively increased lung cancer cell death ($p < 0.05$) (Fig. 6).

PT-262 does not alter the p53 protein expression in the p53-wild type lung cancer cells, and induces cytotoxicity in the p53-null lung cancer cells

Immunoblot analysis showed that treatment with 2–20 μM for 24 h PT-262 did not significantly induce the protein expression of p53 and p21 in the p53-wild type A549 cells (Fig. 7a). As shown in Fig. 7b, PT-262 (2–20 μM for 24 h) decreased the cell viability via a concentration-dependent manner in the p53-null H1299 lung cancer cells. The IC_{50} value of PT-262 toward H1299 cells was approximate at 5 μM, which was similar to A549 cells.

PT-262 induces the accumulation of G_2/M phases in both the p53-wild type and p53-null lung cancer cells, and inhibits the phosphorylation of CDC2 proteins

As shown in Fig. 8a, PT-262 (10 μM for 24 h) significantly decreased the G_1 fractions while increased the G_2/M fractions in both A549 and H1299 cells. To examine the cell cycle-regulated protein expression, the cells were subjected to Western blot analysis. ERK-2 protein was used as an internal control protein. The total CDC2 protein levels were not markedly altered by treatment with PT-262 (Fig. 8b). However, PT-262 (10–20 μM for 24 h) decreased the

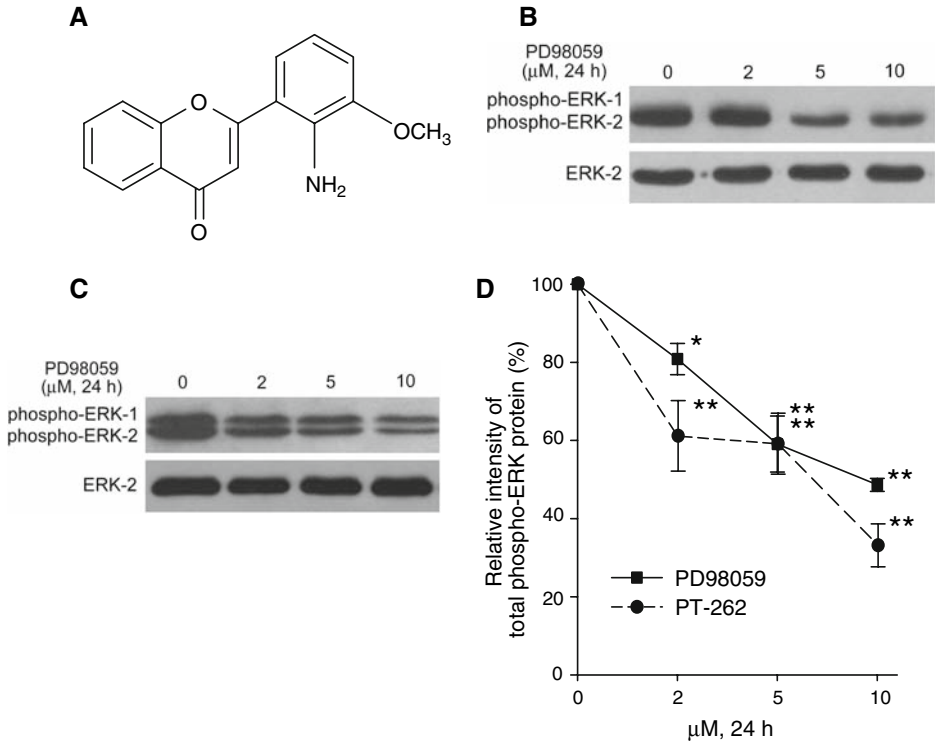

Fig. 5 Effect of a specific MEK1/2 inhibitor, PD98059, and PT-262 on the inhibition of ERK phosphorylation in lung carcinoma cells. **a** The chemical structure of PD98059. **b** A549 cells were treated with 0–50 μM PD98059 for 24 h. **c** A549 cells were treated with 0–10 μM PT-262 for 24 h. At the end of treatment, the total protein extracts were subjected to Western blot analysis. **d** The relative protein intensity was quantified Western blot. Results were obtained from 3 to 4 experiments and the *bar* represents mean ± S.E. $p < 0.05$ (*) and $p < 0.01$ (**), indicates significant differences between control and PT-262 or PD98059 treated samples

protein levels of cyclin B1 and phospho-CDC2 at Thr14, Tyr15, and Thr161 via a concentration-dependent manner in A549 cells (Fig. 8b). PT-262 also reduced the protein levels of cyclin B1 and phospho-CDC2 proteins in H1299 cells (data not shown). Moreover, treatment with 2–20 μM PT-262 for 24 h did not alter the expression of cyclin D1 proteins (Fig. 8b).

Discussion

The derivatives of 5,8-quinolinediones have been shown to inhibit the cell proliferation in human cancer cells; however, these compounds possess the different mechanisms and act on different targets for their anticancer activity [5–7]. LY83583, a derivative of 5,8-quinolinedione, blocks the cell proliferation by inhibiting guanylyl cyclase in tumor cells [5, 6]. NSC 663284, an inhibitor of CDC25 protein phosphatases, induces the cell cycle arrest of cancer cells [7]. PT-262 suppresses the protein phosphorylation of ERK in lung cancer cells. The effectiveness of PT-262 on the inhibition of ERK phosphorylation was at lower concentration levels (2–10 μM). PD98059 is a well-known MEK1/2 inhibitor for the repression of ERK phosphorylation. However, PT-262 did not directly bind to recombinant human MEK1 protein by in vitro binding assay and MALDI/TOF-MS analysis (unpublished data). We suggest that PT-262 may not directly inhibit MEK1/2 kinases. Nonetheless, combination of PD98059 and PT-262 additively increased cytotoxicity in lung cancer cells. It has been shown that the activation of ERK exerts the cell proliferation and anti-apoptosis [12, 13]. We suggest that the suppression of ERK phosphorylation by PT-262 may result in the proliferation inhibition and apoptosis of the human lung cancer cells. However, the mechanisms of PT-262-inhibited ERK signal pathway need further investigation.

Anticancer agents exert their activity through the induction of apoptotic pathways or the blockade of survival pathways in tumor cells [6, 9, 10, 18, 27, 28]. PT-262 induced the decrease of mitochondrial membrane potential and increased the activation of caspase-3 in lung cancer cells. The loss of mitochondrial membrane potential has been indicated mitochondrial dysfunction and subsequent apoptotic event [29, 30]. Interestingly, PT-262 did not alter the p53 protein expression and its downstream protein p21. Moreover, the cytotoxicity and cell arrest were increased by PT-262 in both the p53-wild type and -null lung cancer cells. The p53-null lung cancer cells were displayed similar the IC_{50} value (~5 μM) of cytotoxicity by compared with the p53-wild type lung cancer cells. These findings indicate that PT-262 induces the cell cycle arrest and apoptosis via a p53-independent manner. It is well established that the numerous cancers are caused by the mutations of p53. The loss of functional p53 in cancer cells may resist to chemotherapy and radiotherapy of cancers. Thus, PT-262 is a potential developing anticancer drug, which is still effective on the p53-mutational cancers.

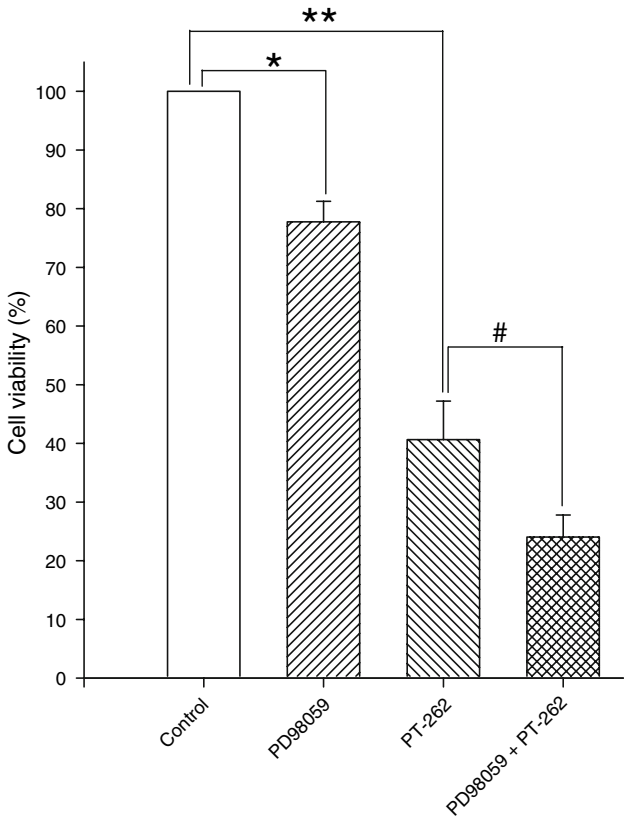

Fig. 6 Effect of a specific MEK1/2 inhibitor, PD98059, on the PT-262-induced cytotoxicity in lung carcinoma cells. The cells were pre-treated with 50 μM PD98059 for 2 h prior to exposure to 8 μM PT-262 for 24 h. After treatment, the cells were washed twice with PBS, and were re-cultured in fresh medium for 48 h. The cell viability was measured by MTT assay. The *bar* represents the mean ± S.E. $^{\#}p < 0.05$ indicates between control and PT-262 treated samples. $^{*}p < 0.05$ indicates significant differences between PT-262 alone and pre-treatment with PD98059

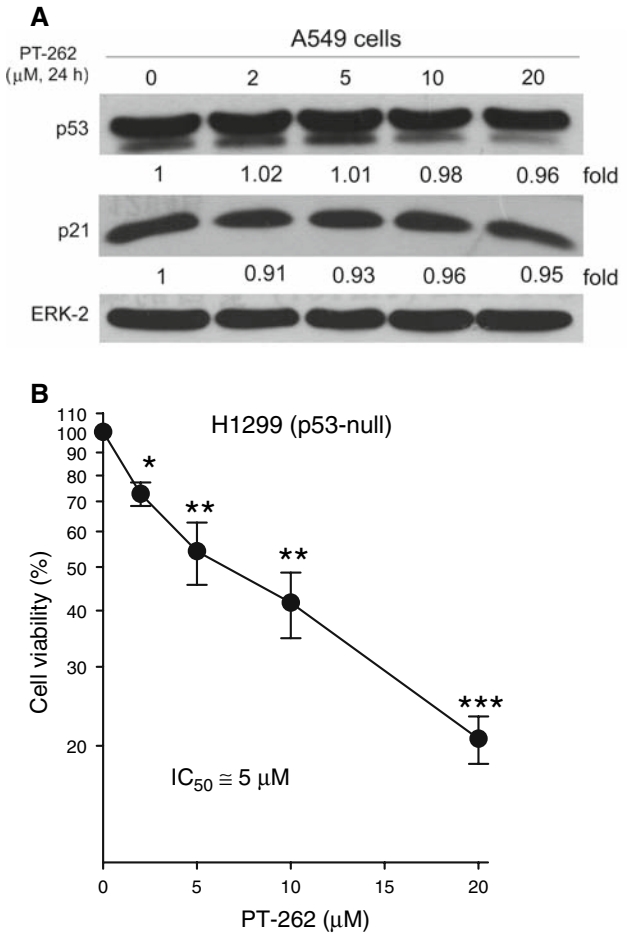

Fig. 7 Effect of PT-262 on the cytotoxicity in the p53-null H1299 lung cancer cells and the p53 protein expression in the p53-wild type A549 cells. **a** A549 cells were treated with 0–20 μM PT-262 for 24 h. After drug treatment, the total protein extracts were subjected to Western blot analysis. The relative fold of protein intensity under each treatment was from the average of three independent experiments. **b** H1299 cells were treated with 2–20 μM PT-262 for 24 h. After treatment, the cells were washed twice with PBS, and were re-cultured in fresh medium for 48 h. The cell viability was measured by MTT assay. Results were obtained from three experiments and the *bar* represents the mean ± S.E. $p < 0.05$ (*) and $p < 0.01$ (**), indicate significant difference between the control and PT-262 treated samples

The interaction of CDC2 and cyclin B1 plays an important role in the mitotic progression [21, 22]. Activation of CDC2 is through the phosphorylation of Thr161 by CDC2 activating kinase (CAK) and the dephosphorylation of Thr14 and Tyr15 by CDC25C phosphatase [31]. NSC 663284 has been shown to inhibit the activity of CDC25 protein phosphatases and blocks the proliferation of tumor cells [3, 7]. Moreover, NSC 663284 blocks the CDC25C phosphatase resulting in the decrease of CDC2 kinase activity for inducing cell cycle arrest [7]. We found that PT-262 reduced the protein levels of cyclin B1 and increased the G_2/M arrest in lung carcinoma cells. Interestingly, the phosphorylated sites of CDC2 at Thr14, Tyr15, and Thr-161 were inhibited by PT-262. Comparing with NSC 663284, PT-262 shows a different role on the regulation on CDC2 and may be not mediated by the inhibition of CDC25C. Furthermore, PT-262 reduced the levels of phospho-CDC2 and cyclin B1 proteins in both the p53-wild type and p53-null lung cancer cells. These observations suggest that the suppression of cyclin B1 protein expression and the disruption of CDC2 phosphorylation by PT-262 participate in the cell cycle arrest and growth inhibition through p53-independent pathway in human lung cancer cells.

In this study, the novel synthetic compounds of 5,8-quinolinedione derivatives or analogues were compared by cytotoxicity assay toward to lung cancer cells. Among these new synthetic compounds, PT-262 is the most potent to induce lung cancer cell death. It has been shown that the cytotoxicity of vitamin K_3 and related quinines is the direct arylation of cellar thiols, leading to the inhibition of sulfhydryl-dependent proteins [32–36]. A chloride substituent and an amino group leads to a considerable perturbation of the

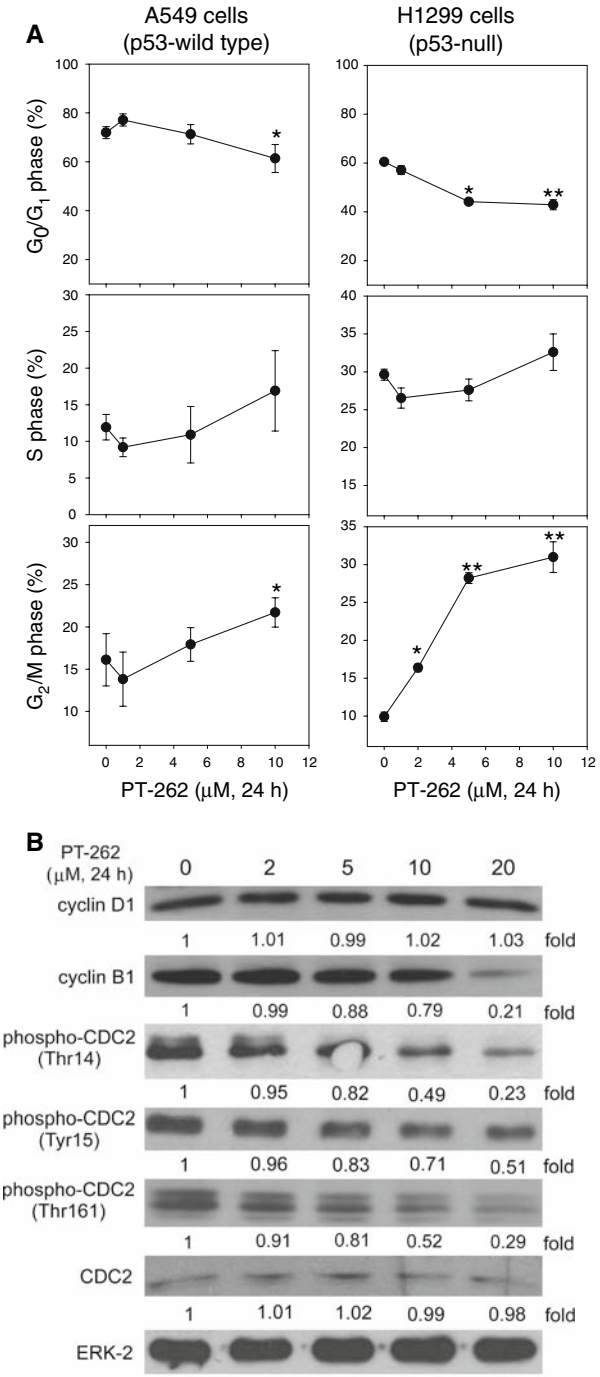

Fig. 8 Effect of PT-262 on the cell cycle progression in the p53-wild type and p53-null lung carcinoma cells. **a** A549 and H1299 cells were treated with 0–10 μM PT-262 for 24 h. The fields of G_1, S, and G_2/M populations were gated for analysis of the cell cycle progression in flow cytometer. The percentage of cell cycle phases was quantified by a ModFit LT software. The data represented the average values from 3 to 4 experiments. The *bar* represents the mean ± S.E. $p < 0.05$ (*) and $p < 0.01$ (**), indicate significant differences between control and PT-262 treated samples in A549 or H1299 cells. **b** The cells were treated with 0–20 μM PT-262 for 24 h. After drug treatment, the total protein extracts were subjected to Western blot analysis. The relative fold of protein intensity under each treatment was from the average of 3–4 independent experiments

electron distribution in heteronaphthoquinones and that this electrostatic effect is likely to provide a better match for the complementary surface in the enzyme binding pocket. We suggest that the unique chemical structure of PT-262 by the existence and position of chloride could therefore represent a specific for the electronic configuration, which is necessary to achieve strong protein inhibition and induces cancer cell death. Nevertheless, the precise chemical reactions of bio-molecules between PT-262 need further examination.

In conclusion, we develop a new synthetic compound, which affects on the apoptotic induction and the cell cycle arrest via a p53-independent pathway in human lung cancer cells. It is an important new modality of anticancer mechanism from the derivatives of 5,8-quinolinediones through the blockade of ERK and CDC2 phosphorylation.

Acknowledgments This work was supported by grant from NSC 96-2311-B-320-006-MY3.

References

1. Yoon E, Choi HY, Shin KJ, Yoo KH, Chi DI, Kim DJ (2000) The regioselectivity in the reaction of 6,7-dihaloquinoline-5,8-diones with amine nucleophiles in various solvents. Tetrahedron Lett 41:7475–7480
2. Boger DL, Yasuda M, Mitscher LA, Drake SD, Kitos PA, Thompson SC (1987) Streptonigrin and lavendamycin partial structures. Probes for the minimum, potent pharmacophore of streptonigrin, lavendamycin, and synthetic quinoline-5,8-diones. J Med Chem 30:1918–1928
3. Pu L, Amoscato AA, Bier ME, Lazo JS (2002) Dual G1 and G2 phase inhibition by a novel, selective Cdc25 inhibitor 7-chloro-6-(2-morpholin-4-ylethylamino)-quinoline-5,8-dione. J Biol Chem 277:46877–46885
4. Fang Y, Linardic CM, Richardson DA, Cai W, Behforouz M, Abraham RT (2003) Characterization of the cytotoxic activities of novel analogues of the antitumor agent, lavendamycin. Mol Cancer Ther 2:517–526
5. Lee YS, Wurster RD (1995) Mechanism of potentiation of LY83583-induced growth inhibition by sodium nitroprusside in human brain tumor cells. Cancer Chemother Pharmacol 36:341–344
6. Lodygin D, Menssen A, Hermeking H (2002) Induction of the Cdk inhibitor p21 by LY83583 inhibits tumor cell proliferation in a p53-independent manner. J Clin Invest 110:1717–1727
7. Lazo JS, Aslan DC, Southwick EC, Cooley KA, Ducruet AP, Joo B, Vogt A, Wipf P (2001) Discovery and biological evaluation of a new family of potent inhibitors of the dual specificity protein phosphatase Cdc25. J Med Chem 44:4042–4049
8. Wall NR, O'Connor DS, Plescia J, Pommier Y, Altieri DC (2003) Suppression of survivin phosphorylation on Thr34 by flavopiridol enhances tumor cell apoptosis. Cancer Res 63:230–235
9. Tamura K, Southwick EC, Kerns J, Rosi K, Carr BI, Wilcox C, Lazo JS (2000) Cdc25 inhibition and cell cycle arrest by a synthetic thioalkyl vitamin K analogue. Cancer Res 60:1317–1325
10. Kuo CC, Hsieh HP, Pan WY, Chen CP, Liou JP, Lee SJ, Chang YL, Chen LT, Chen CT, Chang JY (2004) BPR0L075, a novel synthetic indole compound with antimitotic activity in human cancer cells, exerts effective antitumoral activity in vivo. Cancer Res 64:4621–4628

11. Waskiewicz AJ, Cooper JA (1995) Mitogen and stress response pathways: MAP kinase cascades and phosphatase regulation in mammals and yeast. Curr Opin Cell Biol 7:798–805
12. Mansour SJ, Matten WT, Hermann AS, Candia JM, Rong S, Fukasawa K, Vande Woude GF, Ahn NG (1994) Transformation of mammalian cells by constitutively active MAP kinase kinase. Science 265:966–970
13. Marais R, Marshall CJ (1996) Control of the ERK MAP kinase cascade by Ras and Raf. Cancer Surv 27:101–125
14. Sawhney RS, Cookson MM, Omar Y, Hauser J, Brattain MG (2006) Integrin alpha2-mediated ERK and calpain activation play a critical role in cell adhesion and motility via focal adhesion kinase signaling: identification of a novel signaling pathway. J Biol Chem 281:8497–8510
15. Bates S, Vousden KH (1996) p53 in signaling checkpoint arrest or apoptosis. Curr Opin Genet Dev 6:12–18
16. Levine AJ (1997) p53, the cellular gatekeeper for growth and division. Cell 88:323–331
17. Hofseth LJ, Hussain SP, Harris CC (2004) p53: 25 years after its discovery. Trends Pharmacol Sci 25:177–181
18. Brantley-Finley C, Lyle CS, Du L, Goodwin ME, Hall T, Szwedo D, Kaushal GP, Chambers TC (2003) The JNK, ERK and p53 pathways play distinct roles in apoptosis mediated by the antitumor agents vinblastine, doxorubicin, and etoposide. Biochem Pharmacol 66:459–469
19. Piao W, Yoo J, Lee DK, Hwang HJ, Kim JH (2001) Induction of G(2)/M phase arrest and apoptosis by a new synthetic anti-cancer agent, DW2282, in promyelocytic leukemia (HL-60) cells. Biochem Pharmacol 62:1439–1447
20. Chao JI, Kuo PC, Hsu TS (2004) Down-regulation of survivin in nitric oxide-induced cell growth inhibition and apoptosis of the human lung carcinoma cells. J Biol Chem 279:20267–20276
21. Fang F, Newport JW (1991) Evidence that the G1-S and G2-M transitions are controlled by different cdc2 proteins in higher eukaryotes. Cell 66:731–742
22. King RW, Jackson PK, Kirschner MW (1994) Mitosis in transition. Cell 79:563–571
23. Han Z, Chatterjee D, He DM, Early J, Pantazis P, Wyche JH, Hendrickson EA (1995) Evidence for a G2 checkpoint in p53-independent apoptosis induction by X-irradiation. Mol Cell Biol 15:5849–5857
24. Lock RB, Ross WE (1990) Inhibition of p34cdc2 kinase activity by etoposide or irradiation as a mechanism of G2 arrest in Chinese hamster ovary cells. Cancer Res 50:3761–3766
25. Jordan MA, Toso RJ, Thrower D, Wilson L (1993) Mechanism of mitotic block and inhibition of cell proliferation by taxol at low concentrations. Proc Natl Acad Sci USA 90:9552–9556
26. Kuo PC, Liu HF, Chao JI (2004) Survivin and p53 modulate quercetin-induced cell growth inhibition and apoptosis in human lung carcinoma cells. J Biol Chem 279:55875–55885
27. Ling YH, Yang Y, Tornos C, Singh B, Perez-Soler R (1998) Paclitaxel-induced apoptosis is associated with expression and activation of *c-Mos* gene product in human ovarian carcinoma SKOV3 cells. Cancer Res 58:3633–3640
28. Johnstone RW, Ruefli AA, Lowe SW (2002) Apoptosis: a link between cancer genetics and chemotherapy. Cell 108:153–164
29. Wijnhoven SW, Sonneveld E, Kool HJ, van Teijlingen CM, Vrieling H (2003) Chemical carcinogens induce varying patterns of LOH in mouse T-lymphocytes. Carcinogenesis 24:139–144
30. Isenberg JS, Klaunig JE (2000) Role of the mitochondrial membrane permeability transition (MPT) in rotenone-induced apoptosis in liver cells. Toxicol Sci 53:340–351
31. Pines J (1999) Cell cycle. Checkpoint on the nuclear frontier. Nature 397:104–105
32. Gant TW, Rao DN, Mason RP, Cohen GM (1988) Redox cycling and sulphydryl arylation; their relative importance in the mechanism of quinone cytotoxicity to isolated hepatocytes. Chem Biol Interact 65:157–173
33. Ross D, Thor H, Orrenius S, Moldeus P (1985) Interaction of menadione (2-methyl-1,4-naphthoquinone) with glutathione. Chem Biol Interact 55:177–184
34. Rossi L, Moore GA, Orrenius S, O'Brien PJ (1986) Quinone toxicity in hepatocytes without oxidative stress. Arch Biochem Biophys 251:25–35
35. Wilson I, Wardman P, Lin TS, Sartorelli AC (1987) Reactivity of thiols towards derivatives of 2- and 6-methyl-1,4-naphthoquinone bioreductive alkylating agents. Chem Biol Interact 61:229–240
36. Chen C, Liu YZ, Shia KS, Tseng HY (2002) Synthesis and anticancer evaluation of vitamin K3 analogues. Bioorg Med Chem Lett 12:2729–2732